Journal of Physics: Complexity

Check for updates

PAPER

OPEN ACCESS

RECEIVED
31 March 2026

REVISED
24 June 2026

ACCEPTED FOR PUBLICATION
14 July 2026

PUBLISHED
24 July 2026

Original content from this work may be used under the terms of the Creative Commons Attribution 4.0 licence.

Any further distribution of this work must maintain attribution to the author(s) and the title of the work, journal citation and DOI.

Internal reliability of coupled Kuramoto–Sakaguchi phase oscillators

Arkady Pikovsky[1,*], **Franco Bagnoli**[2,3] **and Stefano Iubini**[4,3]

[1] Institute for Physics and Astronomy, University of Potsdam, Potsdam, Germany
[2] Department of Physics and Astronomy and CSDC, University of Florence, via G. Sansone 1, I-50019 Sesto Fiorentino, Italy
[3] Istituto Nazionale di Fisica Nucleare, Sezione di Firenze, via G. Sansone 1, I-50019 Sesto Fiorentino, Italy
[4] Istituto dei Sistemi Complessi, Consiglio Nazionale delle Ricerche, via Madonna del Piano 10, I-50019 Sesto Fiorentino, Italy
[*] Author to whom any correspondence should be addressed.

E-mail: pikovsky@uni-potsdam.de

Keywords: Kuramoto–Sakaguchi model, reliability, transversal Lyapunov exponent, synchronization

Abstract

The notion of internal reliability in dynamical networks describes whether replicas of a particular unit follow the dynamics of the reference unit. Reliability and anti-reliability can be quantified by the transversal Lyapunov exponents. We study phase oscillators coupled via Kuramoto–Sakaguchi-type interactions. Already the simplest solvable system of two oscillators demonstrates nontrivial reliability properties. We present numerical evidence of reliability and anti-reliability in small networks with a uniform distribution of natural frequencies. The dynamics of an ensemble of replicas can be described within the Watanabe–Strogatz theory, which predicts symmetry of the transversal Lyapunov exponents for replica-attractor and replica-repeller.

1. Introduction

Synchronization by common noise means that the states of two identical nonlinear systems driven by the same noise converge and eventually coincide despite different initial conditions [1]. In neurosciences, this effect is called reliability [2–5]. In the reliability setup, one has a single system (a neuron) and applies the same pre-recorded noise signal to it repeatedly, assuming the system's properties remain the same (apart from initial conditions). If repeated driving of a system with the same noise force produces the same response, one calls such a situation reliable, which corresponds to synchronization. Reliability and synchronization by common noise are quantified by the largest Lyapunov exponent of the noise-driven system: a negative Lyapunov exponent means synchronization and reliability, while a positive Lyapunov exponent means sensitivity to initial conditions, desynchronization, and anti-reliability [6]. Remarkably, the same concept under the name of damage spreading has been introduced in the field of Monte-Carlo simulations of models with discrete state space, like the Ising model or probabilistic cellular automata [7–9]. Here, common noise means that the same sequence of random numbers is used in the Monte-Carlo steps for two systems that differ only by an initial state. Synchronization (reliability) in this setup is called 'healing' (damage disappears), while the absence of synchrony (anti-reliability) is referred to as a chaotic situation. Although the usual notion of the Lyapunov exponent is not applicable for systems with discrete states, one can use Boolean derivatives to properly define the Lyapunov exponent in the realm of damage spreading [10].

If one replaces noisy driving by a chaotic one, resulting from a chaotic dynamical system, then synchronization by common noise and reliability coincide with the notion of generalized synchronization of chaos [11–15]. Generalized synchronization setup is illustrated in figure 1(a), where the driving unit $\boldsymbol{x}_1$ not only drives the unit $\boldsymbol{x}_2$, but also its three replicas $\boldsymbol{X}_{2,1}, \boldsymbol{X}_{2,2}, \boldsymbol{X}_{2,3}$. Synchronization occurs if at large times $\boldsymbol{x}_2 = \boldsymbol{X}_{2,1} = \boldsymbol{X}_{2,2} = \boldsymbol{X}_{2,3}$

In a recent paper [16], we extended the notion of reliability to the case where different units are coupled bi-directionally (and not uni-directionally, as in the generalized synchronization setup), see figure 1. One chooses one subunit of a complex network (we call this unit a prototype) and prepares one or

© 2026 The Author(s). Published by IOP Publishing Ltd

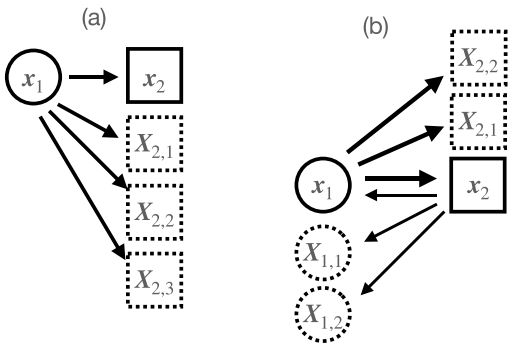

Figure 1. (a) A sketch of the generalized synchronization problem; (b) a sketch of the internal reliability one. In the generalized synchronization, there is a unidirectional coupling $1 \to 2$, while in the internal reliability setup the coupling is bidirectional $1 \leftrightarrow 2$. The driving force of replicas ($\boldsymbol{X}_{k,m}$) is the same as that of the prototype ($\boldsymbol{x}_k$).

several identical replicas of this unit. These replicas receive the same input from the rest of the network as the prototype receives, but they do not influence other units and remain 'passive'. The replicas can have different initial states. As an example, we present in figure 1(b) two bidirectionally interacting units $\boldsymbol{x}_1, \boldsymbol{x}_2$, and prepare two replicas of each unit. The replicas of $\boldsymbol{x}_1$ (denoted as $\boldsymbol{X}_{1,1}, \boldsymbol{X}_{1,2}$) are driven by the same force from unit $\boldsymbol{x}_2$ as the unit $\boldsymbol{x}_1$. If the states of the replicas in course of time converge to the state of the prototype (for example, $\boldsymbol{X}_{1,1} \to \boldsymbol{x}_1$, $\boldsymbol{X}_{1,2} \to \boldsymbol{x}_1$), one calls this unit reliable; otherwise, if the states of the replicas remain different from the state of the prototype, one speaks of anti-reliability. We note here that using replicas of certain variables of a chaotic system is a central point of the Pecora–Carroll setup of chaos synchronization [17]. The main difference of our setup in this paper is that here a network of regular oscillators is considered, and the overall dynamics can also be regular and not chaotic.

In this paper, we discuss reliability properties of phase oscillators with a Kuramoto–Sakaguchi (KS)-type coupling [18–21]. After presenting a general formalism of internal reliability in section 2, we study in detail the case of two coupled oscillators in section 3. Here, the problem can be solved analytically. After that, in section 4, we discuss reliability properties of larger networks, employing numerical simulations and the Watanabe–Strogatz (WS) theory [22, 23]. The results are discussed in section 5.

2. General notion of internal reliability

In this section, we shortly introduce the notion of internal reliability, following recent paper [16].

2.1. Replicas and their stability

Consider a system of N coupled units $\boldsymbol{x}_j$, $j = 1, \ldots, N$, described by coupled dynamical equations

$$\dot{\boldsymbol{x}}_j = \boldsymbol{F}_j\left(\boldsymbol{x}_j; \boldsymbol{x}_{l\neq j}\right), \quad j = 1, \ldots, N. \tag{1}$$

Note that all units can be completely different (i.e. they have different dimensions and different dynamics). In this paper, we assume dissipative dynamics in equation (1), and suppose that at $t = 0$ the state $\boldsymbol{x}_j(0)$ is on an attractor.

Let us fix some unit k and make at time $t = 0$ several replicas, $\boldsymbol{X}_{k,m}(0)$, of it (see sketch in figure 1(b), where replicas are depicted with dashed lines). We call the replicated unit $\boldsymbol{x}_k$ the prototype. These replicas receive the same input from other units as $\boldsymbol{x}_k$ does, so that their dynamics is

$$\dot{\boldsymbol{X}}_{k,m} = \boldsymbol{F}_k\left(\boldsymbol{X}_{k,m}; \boldsymbol{x}_{l\neq k}\right), \quad m = 1, \ldots, M. \tag{2}$$

The system described by equations (1) and (2) is a skew system, where replicas are forced by the units $\boldsymbol{x}_j$, but not vice versa. It is evident that if the initial state of a replica coincides with its prototype, i.e. $\boldsymbol{X}_{k,m}(0) = \boldsymbol{x}_k(0)$, then for all $t > 0$ their states also coincide $\boldsymbol{X}_{k,m}(t > 0) = \boldsymbol{x}_k(t > 0)$. However, if a replica does not coincide with the prototype initially, i.e. $\boldsymbol{X}_{k,m}(0) \neq \boldsymbol{x}_k(0)$, different scenarios are possible.

If all or almost all replicas converge to the prototype $|\boldsymbol{X}_{k,m}(t) - \boldsymbol{x}_k(t)| \to 0$ as $t \to \infty$, we call the unit k **reliable**. If all or almost all replicas do not converge to the corresponding prototype, we call such a unit **anti-reliable**.

In general, there are more possibilities related to 'multi-stability': one can imagine situations where some replicas of the same prototype (i.e. replicas that have the same index k but different index m)

converge to the corresponding prototype while others do not. For example, for a setup presented in figure 1(b), multistability in replicas occurs if $\boldsymbol{X}_{2,1}$ converges to $\boldsymbol{x}_2$, while $\boldsymbol{X}_{2,2}$ remains at a finite distance to $\boldsymbol{x}_2$. However, as we show below, such behavior cannot occur in phase oscillators with KS-type coupling, and we will not further elaborate on these possibilities.

It is convenient to denote a trajectory, to which replicas driven by equation (2) converge, with the term *replica-attractor*. Because generally the forcing in equation (2) is irregular, this attractor is not a set in the phase space of replicas $\boldsymbol{X}$, but a trajectory to which trajectories with other initial conditions converge. A similar definition of a random attractor (sometimes called 'pullback attractor') is used for randomly driven systems. In the reliable case, the prototype trajectory coincides with the replica attractor. In the anti-reliable case, the prototype trajectory is unstable. Generally, such a trajectory can be of saddle type, but for one-dimensional units like phase oscillators, there is only one unstable direction. Thus, the prototype is *replica-repeller*, while the replica-attractor is a different trajectory.

To determine whether the replicas converge to the prototype or not, one has to examine their linear stability properties. Let us denote the deviation of a replica $\boldsymbol{X}_k$ from the prototype $\boldsymbol{x}_k$ as $\boldsymbol{u}_k = \boldsymbol{X}_k - \boldsymbol{x}_k$. The equation for this deviation is obtained by subtracting equation (1) from equation (2):

$$\dot{\boldsymbol{u}}_k = \dot{\boldsymbol{X}}_k - \dot{\boldsymbol{x}}_k = \boldsymbol{F}_k(\boldsymbol{X}_k; \boldsymbol{x}_{l\neq k}) - \boldsymbol{F}_k(\boldsymbol{x}_k; \boldsymbol{x}_{l\neq k}) = \boldsymbol{F}_k(\boldsymbol{x}_k + \boldsymbol{u}_k; \boldsymbol{x}_{l\neq k}) - \boldsymbol{F}_k(\boldsymbol{x}_k; \boldsymbol{x}_{l\neq k}) \ .$$

Considering infinitely small deviations $\boldsymbol{u}_k$, we obtain after linearization

$$\dot{\boldsymbol{u}}_k = \frac{\partial}{\partial \boldsymbol{x}_k} \boldsymbol{F}_k(\boldsymbol{x}_k; \boldsymbol{x}_{l\neq k})\, \boldsymbol{u}_k \ . \tag{3}$$

The linear system of equation (3), where states $\{\boldsymbol{x}_j\}$ evolve according to equation (1), defines transversal Lyapunov exponents [24] (their number is determined by the dimension of variable $\boldsymbol{u}_k$), and it is enough to look at the largest of them, which determines the asymptotic growth rate of the perturbation $|\boldsymbol{u}_k(t)| \sim \exp(\lambda_k t)$. If the largest transversal Lyapunov exponent (LTLE) λ_k is positive, the trajectory $\boldsymbol{x}_k(t)$ is unstable in replica phase space, and this unit is anti-reliable. If the LTLE is negative, then the unit is reliable. Note that the LTLE depends on the index k; as we will see below, there are situations where some units are reliable and some anti-reliable (it can happen that all units are reliable or all units are anti-reliable, but we never observed the latter situation for phase oscillators).

Similarly to the stability of the prototype, we can quantify the stability of the replica-attractor (qualitatively, this attractor is always stable due to the definition). Suppose that different replicas converge to an attracting trajectory $\boldsymbol{X}_k(t)$. Denoting $\boldsymbol{w}_k$ an infinitesimal difference between two replicas close to the replica-attractor, we obtain the evolution

$$\dot{\boldsymbol{w}}_k = \frac{\partial}{\partial \boldsymbol{X}_k} \boldsymbol{F}_k(\boldsymbol{X}_k; \boldsymbol{x}_{l\neq k})\, \boldsymbol{w}_k \ . \tag{4}$$

Here states $\boldsymbol{X}_k, \boldsymbol{x}_{j\neq k}$ evolve according to the system of equations (1) and (2). The largest Lyapunov exponent Λ_{attr} of equation (4) determines the rate with which $\boldsymbol{w}_k$ decays: $|\boldsymbol{w}_k(t)| \sim \exp[\Lambda_{\text{attr}} t]$, with $\Lambda_{\text{attr}} < 0$.

2.2. Reliability and inference of the unit's state and parameters

In this section, we shortly discuss the importance of reliability in a particular technique of recovering a unit's properties from the observations. Suppose that in the system of equation (1), we observe all the units except unit k. If we know the equations of motion of $\boldsymbol{x}_k$, we can try to solve equation (2) starting from arbitrary initial conditions, in the hope that this solution $\boldsymbol{X}_k(t)$ after some transient will reproduce the true evolution of $\boldsymbol{x}_k(t)$. As it follows from the definitions of section 2, this is possible only if reliability holds. In an anti-reliable situation, such a method fails.

3. Reliability of two coupled phase oscillators

The main topic of this paper is the exploration of the reliability properties of phase oscillators with a KS type coupling. The case of Kuramoto coupling has been considered in [16], with emphasis on large ensembles. Here, we focus on a small number of coupled oscillators.

In this section, we consider the simplest possible setup of two coupled oscillators. The remarkable feature is that the reliability properties can be determined analytically.

3.1. Basic equations

We restrict our attention to the simplest case of pure main harmonic coupling. Then, the general equations for coupled phase oscillators $\tilde{x},\tilde{y}$ read

$$\begin{aligned}\frac{\mathrm{d}}{\mathrm{d}t}\tilde{x}&=\tilde{\omega}_x+\tilde{a}_x\sin\left(\tilde{y}-\tilde{x}-\tilde{\alpha}_x\right)\,,\\ \frac{\mathrm{d}}{\mathrm{d}t}\tilde{y}&=\tilde{\omega}_y+\tilde{a}_y\sin\left(\tilde{x}-\tilde{y}-\tilde{\alpha}_y\right)\,.\end{aligned}\tag{5}$$

There are six parameters: two natural frequencies $\tilde{\omega}_x,\tilde{\omega}_y$, two coupling strengths $\tilde{a}_x,\tilde{a}_y$, and two phase shifts $\tilde{\alpha}_x,\tilde{\alpha}_y$. With a transformation $\tilde{x}=(\tilde{\omega}_x+\tilde{\omega}_y)/2\,t+(\tilde{\alpha}_x-\tilde{\alpha}_y)/2+x$, $\tilde{y}=(\tilde{\omega}_x+\tilde{\omega}_y)/2\,t+y$, one can make the natural frequencies equal in modulus $\pm(\tilde{\omega}_x-\tilde{\omega}_y)/2$, and the phase shifts equal to $\alpha=(\tilde{\alpha}_x+\tilde{\alpha}_y)/2$. Assuming for definiteness that $\tilde{\omega}_x>\tilde{\omega}_y$, we rescale time by the factor $(\tilde{\omega}_x-\tilde{\omega}_y)/2$ and obtain a system containing three parameters only:

$$\begin{aligned}\dot{x}&=1+\varepsilon\cos\beta\sin\left(y-x-\alpha\right)\,,\\ \dot{y}&=-1+\varepsilon\sin\beta\sin\left(x-y-\alpha\right)\,.\end{aligned}\tag{6}$$

Here instead of coupling constants $\tilde{a},\tilde{b}$, we introduced the overall coupling strength ε and the coupling asymmetry parameter β according to $2\tilde{a}_x/(\tilde{\omega}_x-\tilde{\omega}_y)=\varepsilon\cos\beta$, $2\tilde{a}_y/(\tilde{\omega}_x-\tilde{\omega}_y)=\varepsilon\sin\beta$. It is convenient to assume $\varepsilon>0,\beta\in(-\pi,\pi),\alpha\in(-\pi,\pi)$. The cases $\beta=0,\pi$ (where $\tilde{a}_y=0$) or $\beta=\pm\pi/2$ (where $\tilde{a}_x=0$) correspond to unidirectional coupling, the case $\beta=\pi/4$ corresponds to symmetric coupling (where $\tilde{a}_x=\tilde{a}_y$).

3.2. Replicas and transversal Lyapunov exponents

Together with x,y we consider replicas X of x and Y of y, which are driven by the prototypes:

$$\begin{aligned}\dot{X}&=1+\varepsilon\cos\beta\sin\left(y-X-\alpha\right)\,,\\ \dot{Y}&=-1+\varepsilon\sin\beta\sin\left(x-Y-\alpha\right)\,.\end{aligned}\tag{7}$$

For small deviations $\delta_x=X-x$, $\delta_y=Y-y$ we have linear equations

$$\begin{aligned}\dot{\delta}_x&=-\delta_x\left[\varepsilon\cos\beta\cos\left(y-x-\alpha\right)\right]\,,\\ \dot{\delta}_y&=-\delta_y\left[\varepsilon\sin\beta\cos\left(x-y-\alpha\right)\right]\,.\end{aligned}\tag{8}$$

This defines two LTLEs determining the reliability of phases x,y:

$$\begin{aligned}\lambda_x&=-\left\langle\varepsilon\cos\beta\cos\left(y-x-\alpha\right)\right\rangle\,,\\ \lambda_y&=-\left\langle\varepsilon\sin\beta\cos\left(x-y-\alpha\right)\right\rangle\,.\end{aligned}\tag{9}$$

3.3. Dynamics and analytic calculation of LTLEs

Equations (6) can be solved by introducing the phase difference $z=x-y$, which obeys a first-order equation

$$\dot{z}=2-\varepsilon A\sin\left(z+\phi\right)\,,\tag{10}$$

where $A\cos\phi=\cos\alpha(\cos\beta+\sin\beta)$, $A\sin\phi=\sin\alpha(\cos\beta-\sin\beta)$, $A^2=1+\sin2\beta\cos2\alpha$. The dynamics of z is either periodic (if $\varepsilon A<2$) or a fixed point $\bar{z}=\arcsin\frac{2}{\varepsilon A}-\phi$ (if $\varepsilon A\geqslant 2$). Correspondingly, the oscillators are synchronized for $\varepsilon A\geqslant 2$ or are in an asynchronous, quasiperiodic regime for $\varepsilon A<2$.

Thus, the distribution density of z, required for calculation of the LTLEs (9), is

$$\rho(z)=\begin{cases}\delta\left(z-\bar{z}\right) & \varepsilon A\geqslant 2\,,\\ \frac{\sqrt{4-\varepsilon^2A^2}}{2\pi}\frac{1}{2-\varepsilon A\sin(z+\phi)} & \varepsilon A<2\,.\end{cases}\tag{11}$$

Substitution of equation (11) in equation (9) yields LTLEs:

Synchronous case $\varepsilon A\geqslant 2$:

$$\begin{aligned}\lambda_x&=A^{-2}\left[\sin2\beta\sin2\alpha-\sqrt{\varepsilon^2A^2-4}\cos\beta\left(\cos\beta+\sin\beta\cos2\alpha\right)\right]\,,\\ \lambda_y&=-A^{-2}\left[\sin2\beta\sin2\alpha+\sqrt{\varepsilon^2A^2-4}\sin\beta\left(\sin\beta+\cos\beta\cos2\alpha\right)\right]\,.\end{aligned}\tag{12}$$

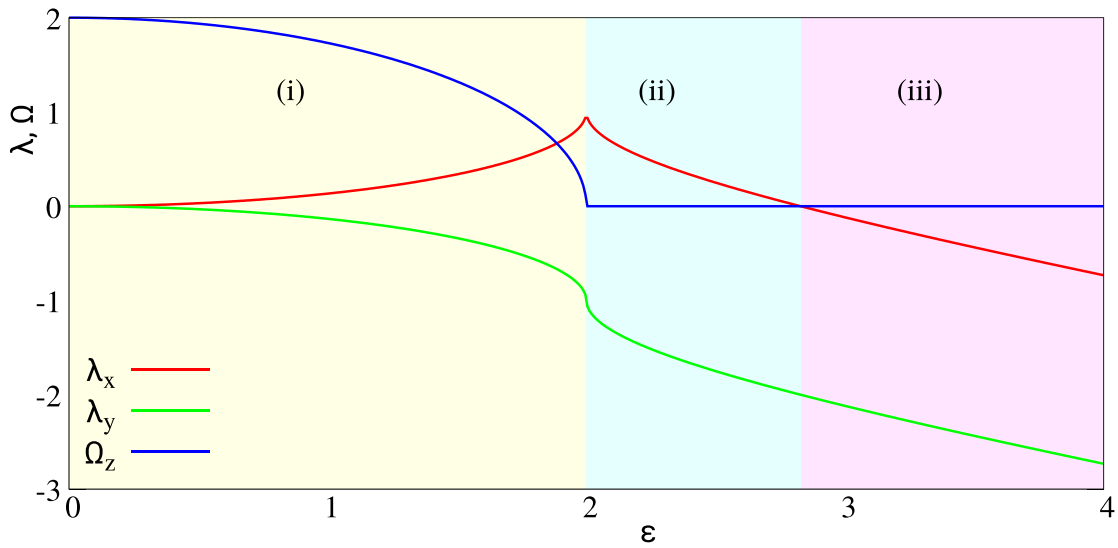

Figure 2. Transversal LEs, equation (14), as functions of the coupling strength. Additionally, we show the frequency difference $\Omega_z = \langle \dot{z} \rangle$ to indicate the synchronization transition at $\varepsilon = 2$. Colored regions indicate different states according to synchrony and reliability properties, as described in the text.

Asynchronous case $\varepsilon A < 2$:

$$\begin{aligned} \lambda_x &= \left(2A^2\right)^{-1} \left(2 - \sqrt{4 - \varepsilon^2 A^2}\right) \sin 2\beta \sin 2\alpha \,, \\ \lambda_y &= -\lambda_x \,. \end{aligned} \tag{13}$$

The result of equation (13) is quite remarkable, as it shows that in the asynchronous state, either both LTLEs vanish (this happens, e.g. for a fully asymmetric coupling with $\beta = 0,\ \pi/2$) or they have opposite signs, i.e. one oscillator is reliable while the other one is not. In the synchronous case, either two LTLEs have different signs, like in the case of asynchrony, or both are negative.

3.4. Reliability properties

Because the system of equation (6) has three parameters, a graphical representation of all possible situations is hardly possible. Therefore, discuss properties of reliability in particular cases.

Kuramoto coupling $\alpha = 0$. In this case, both LTLEs vanish in the asynchronous case at small coupling. In the synchronous regime at strong couplings, the sum of LTLEs is always negative, i.e. they cannot be both positive. The LTLEs have opposite signs if $\sin 2\beta < 0$, i.e. if the coupling coefficients $\tilde{a}_x, \tilde{a}_y$ in equation (5) have opposite signs.

Symmetric coupling $\beta = \pi/4$. In this case, LEs generally do not vanish in both the synchronous and the asynchronous states.

Let us consider, as a representative example, the case $\alpha = \beta = \pi/4$. Then $A = 1$ and the expressions for the LEs are simple:

$$\lambda_x = \begin{cases} \frac{\left(2-\sqrt{4-\varepsilon^2}\right)}{2} & \varepsilon < 2 \,, \\ 1 - \frac{\sqrt{\varepsilon^2-4}}{2} & \varepsilon \geqslant 2 \,, \end{cases} \qquad \lambda_y = \begin{cases} -\frac{\left(2-\sqrt{4-\varepsilon^2}\right)}{2} & \varepsilon < 2 \,, \\ -1 - \frac{\sqrt{\varepsilon^2-4}}{2} & \varepsilon \geqslant 2 \,. \end{cases} \tag{14}$$

We illustrate these LEs in figure 2. One can see that λ_y is always negative, while λ_x is positive for small couplings and becomes negative for $\varepsilon > 2\sqrt{2}$. This means that the oscillator x is anti-reliable in the whole asynchronous domain, and in the synchronous region for small coupling strengths.

We illustrate different regimes in figure 3. In these figures, we show trajectories of prototypes (colored curves) and 20 replicas (gray curves), so that one can easily see which solution the replicas converge to. In all cases, the unit y is reliable. For $\varepsilon = 1$ (regime (i) of figure 2), the dynamics is quasiperiodic and asynchronous; the unit x is antireliable, and the replicas X_m do not converge to the prototype x, while the unit y is reliable and the replicas Y_m converge to the prototype y. The same reliability properties hold for $\varepsilon = 2.2$ (regime (ii) of figure 2), but now the dynamics is synchronous periodic. For $\varepsilon = 3.1$ (regime (iii) of figure 2), the dynamics is synchronous, and both units are reliable.

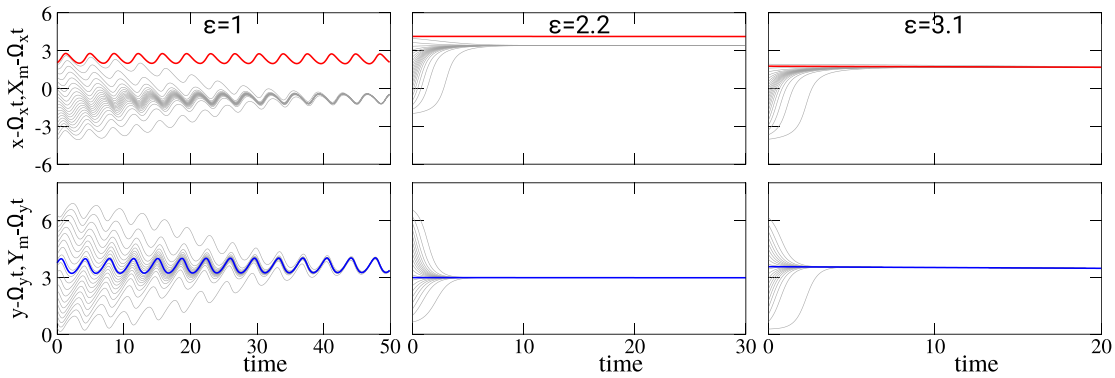

Figure 3. Prototypes (red and blue) and replicas (gray) for three values of coupling strength ε. To enhance visibility, linear-in-time terms $\Omega_x t, \Omega_y t$ are subtracted from all phases on each panel, where $\Omega_x = \langle \dot{x} \rangle$, $\Omega_y = \langle \dot{y} \rangle$ are mean frequencies.

3.5. A simple example

Here we present the simplest example with nontrivial reliability properties. We take two oscillators x, y with equal frequencies, so that in the co-rotating reference frame the frequencies can be set to zero. Suppose that oscillator x attempts to follow y, but y attempts to be in anti-phase with x. In terms of [25, 26], oscillator x is a 'conformist' and oscillators y is a 'contrarian'. For definiteness, suppose that the attraction of x to y is stronger than the repulsion of y from x. Then, the equations for the oscillators, their replicas, and the phase difference $z = x - y$ read:

$$\dot{x} = 2\sin(y - x) \ , \tag{15}$$

$$\dot{y} = -\sin(x - y) \ , \tag{16}$$

$$\dot{X} = 2\sin(y - X) \ , \tag{17}$$

$$\dot{Y} = -\sin(x - Y) \ , \tag{18}$$

$$\dot{z} = -\sin z \, . \tag{19}$$

From equation (19) it follows that conformism wins and two oscillators relax on the stable fixed point $z = 0$, i.e. they synchronize ($x = y$). From equations (17) and (18) it follows that the replica of the conformist also synchronizes ($X = x = y$) and is reliable, while the replica of the contrarian is in anti-phase with its prototype ($Y = y + \pi$) and thus anti-reliable. In the diametrical case of stronger repulsion between x and y, the situation will be opposite: the conformist will be anti-reliable, and the contrarian will be reliable.

4. Reliability in KS ensembles

For three or more coupled oscillators, even if the coupling functions contain the basic harmonics only, there are many different possibilities due to different choices of the natural frequencies, the coupling strengths, and the phase shifts. Therefore, below we restrict our attention to the case of global coupling, in which all coupling strengths and phase shifts are equal. The oscillators differ only by their frequencies, and we will assume a uniform distribution of frequencies: for N units, the set of frequencies is $-1, -1 + 2/(N-1), \ldots, 1$. The example of section 3.4 belongs to this class. The Kuramoto ensemble case with $\alpha = 0$ has been explored in [16]; here we focus on the KS ensemble with $\alpha = \pi/4$, for several representative values of N.

4.1. Transversal exponents

Here we report on reliability properties of the KS ensemble with phase shift $\alpha = \pi/4$:

$$\dot{x}_j = \omega_j + \frac{\varepsilon}{N} \sum_{l \neq j} \sin\left(x_l - x_j - \pi/4\right) \ , \quad j = 1, \ldots, N \, . \tag{20}$$

According to the general expression of equation (3), the dynamics of the transversal perturbation u_k for each unit is one-dimensional. Thus, the LTLE (in fact, here there is only one transversal exponent)

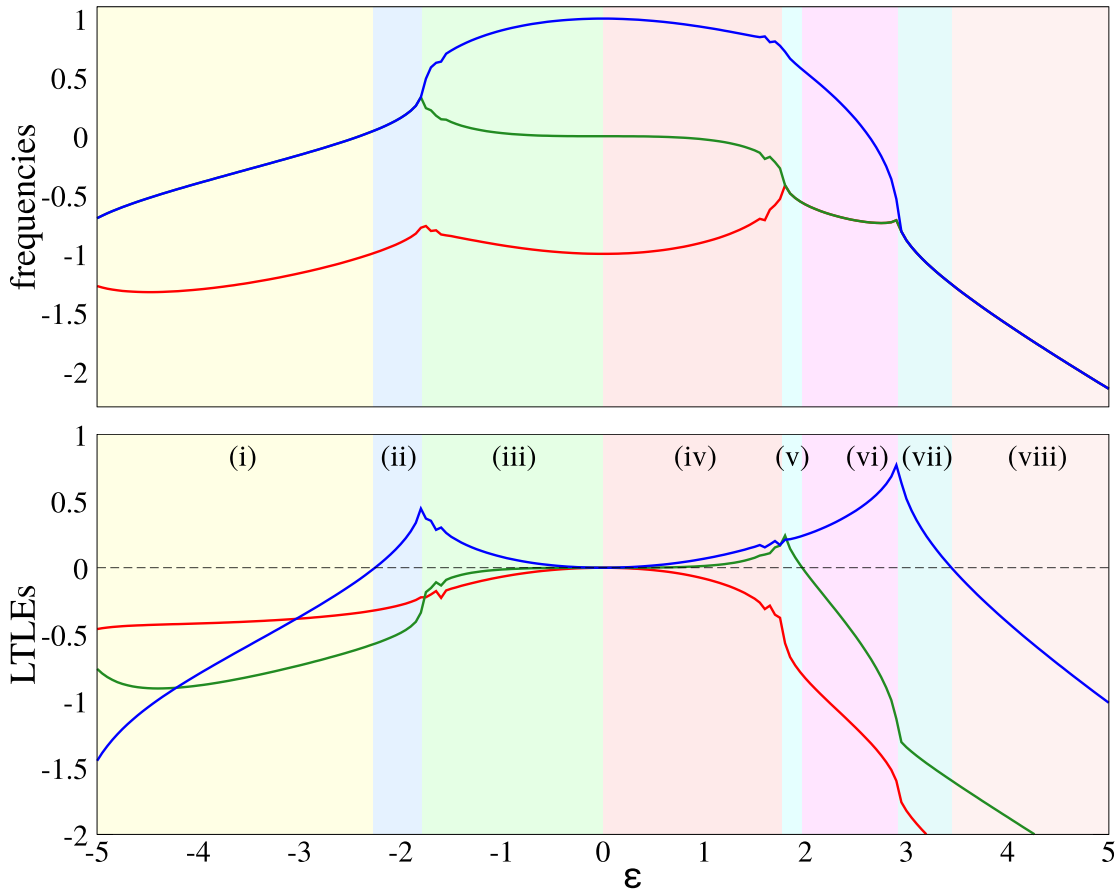

Figure 4. Observed frequencies (upper panel) and LTLEs (bottom panel) for $N = 3$ oscillators with Kuramoto–Sakaguchi coupling (equation (20)). Red, green, and blue lines depict oscillators with natural frequencies -1, 0, 1, respectively. Colored regions indicate different states according to synchrony and reliability properties, as described in detail in the text.

reduces to the time averaging of the corresponding factor:

$$\lambda_k = -\frac{\varepsilon}{N}\sum_{l\neq k}\langle\cos\left(x_l - x_k - \pi/4\right)\rangle\ . \tag{21}$$

The system of two oscillators, analytically solved in section 3.4, belongs to this family (with slightly different normalization of the coupling constant).

We illustrate the case $N = 3$ in figure 4. Here, there are eight different regimes, which can be classified according to properties of synchrony (according to frequencies in the upper panel) and to the properties of reliability (via LTLEs in the bottom panel). Here for small $|\varepsilon|$ all units have different frequencies (regimes (iii),(iv)), for larger $|\varepsilon|$ a two-frequency regime is observed (regimes (i),(ii),(v),(vi)), and for large positive ε all oscillators are synchronized and possess the same frequency (regimes (vii),(viii)). All these states are regular, with the vanishing largest Lyapunov exponent. The oscillator with the lowest natural frequency is reliable for all coupling strengths, the oscillator with the middle natural frequency is anti-reliable for small positive values of ε (regimes (iv),(v)), and the oscillator with the largest natural frequency is anti-reliable both for positive and negative couplings (regimes (ii),(iii),(iv),(v),(vi),(vii)), while the domain of anti-reliability is larger for positive ε. This oscillator is reliable in domains (i),(viii). Similar to the case of two oscillators, figure 2, there is a domain (vii) of coupling strengths around $\varepsilon \approx 3.2$, where in the regime of full synchrony, the unit with the largest natural frequency is anti-reliable.

The cases with larger numbers of units in an ensemble are illustrated in figure 5. The first observation is that in a large domain of coupling strengths, the dynamics is chaotic [27–30], as the presented largest Lyapunov exponent of equation (20) shows (bottom panels). Only for large positive ε, where there is a large cluster of synchronized units with a few having maximal natural frequency that still deviate in the observed frequencies, the dynamics becomes regular. The second observation is that anti-reliability is characteristic for oscillators with larger natural frequencies. So, for $N = 11$, the units $1 \leqslant k \leqslant 4$ are always reliable; units $k = 5, 6$ are anti-reliable in some range of positive couplings; and

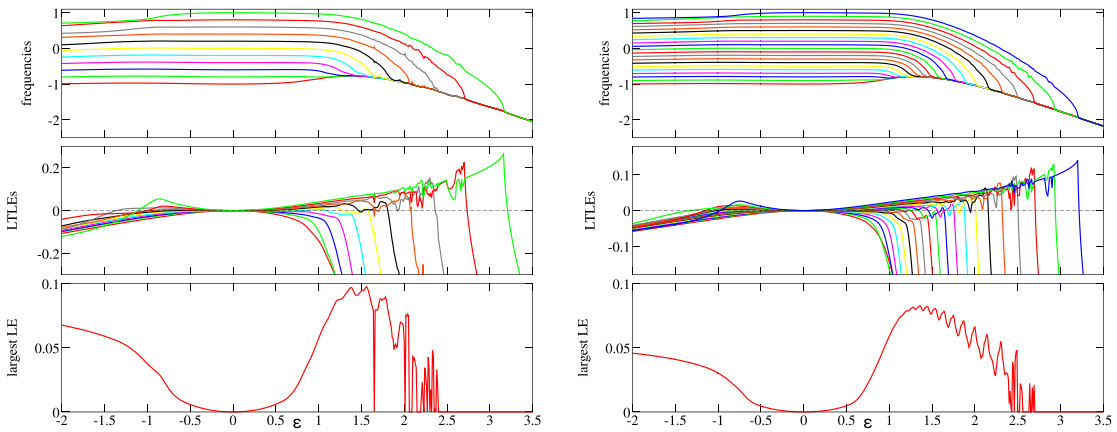

Figure 5. Reliability properties of the KS ensembles, equation (20), with $N = 11$ (left) and $N = 21$ (right). Upper panels: observed frequencies vs ε, showing a synchronization transition at positive ε. Middle panels: LTLEs revealing reliable (negative values) and anti-reliable (positive values) oscillators. Bottom panels: the largest Lyapunov exponent of the dynamics.

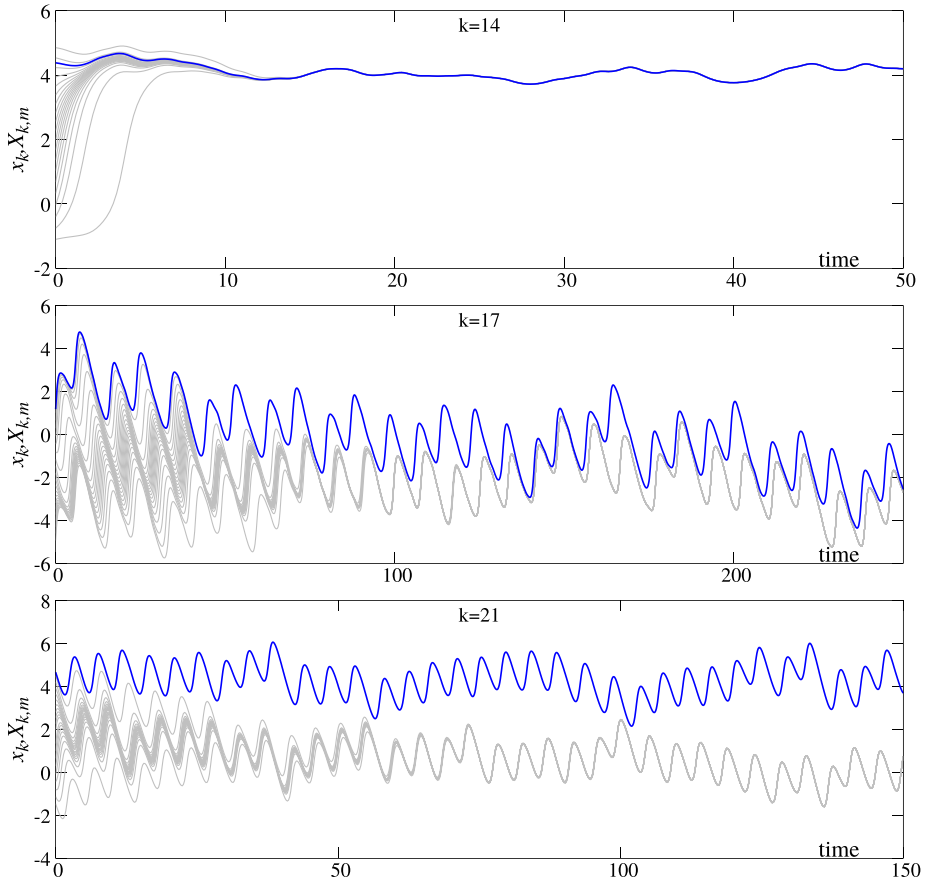

Figure 6. Evolution of the prototypes x_k (blue curves) and of 20 replicas $X_{k,m}$ (gray curves) in the Kuramoto–Sakaguchi model, equation (20), for $\varepsilon = 2$ and $N = 21$. The unit $k = 14$ is reliable, while units $k = 17, 21$ are anti-reliable. For clarity of presentation, from all graphs, the average phase shift $\Omega_k t$ is subtracted.

units $7 \leqslant k \leqslant 11$ are anti-reliable for positive and negative couplings. The third observation is that reliability is not directly related to chaos; anti-reliable and reliable units are observed in both chaotic and regular states.

4.2. Illustration of reliable and anti-reliable dynamics

In figure 6 we illustrate reliable and anti-reliable dynamics in the KS model of equation (20) for $\varepsilon = 2$ and $N = 21$. We show 20 replicas of 3 units: (i) $k = 14$, this unit belongs to the cluster of synchronized

oscillators and is reliable (all replicas $X_{k,m}$ converge to the prototype x_k); (ii) $k=17$, this unit is anti-reliable with relatively small positive transversal LE (all replicas $X_{k,m}$ converge to a trajectory which is different from the prototype x_k but remains relatively close to it); (iii) $k=21$, this unit is strongly anti-reliable (all replicas $X_{k,m}$ converge to a trajectory which is different from the prototype x_k and lies far away from it.).

4.3. Properties of a replica-attractor and a replica-repeller in the KS model

We note that in each panel of figure 6, all the units are driven by the same field, only their initial conditions at $t=0$ differ. The state of the prototype (blue curves) is fixed by the preceding dynamics of the full system of equation (20), while initial states of replicas can be chosen arbitrarily. In all cases, the replicas converge to a single trajectory, which we dub *replica-attractor*. The trajectory of the prototype is also replica-attractor if the transversal LE is negative (case $k=14$ in figure 6), but it is *replica-repeller* if the transversal LE is positive (cases $k=17, k=21$ in figure 6). We stress here that the prototype always belongs to an attractor in the full system, equation (20), thus we use different terms to emphasize that figure 6 illustrates attraction and repulsion in the replica space.

Replica-attractor and replica-repeller in the KS system can be further characterized by virtue of the WS theory [22, 23]. In particular, we use a complex formulation of the WS theory according to [31, 32], and Hamiltonian formulation according to [33].

Here we discuss in detail the dynamics of replicas of a particular unit k in the ensemble, equation (20). For brevity of notations, we omit index k everywhere, and denote the set of replicas as $\varphi_m(t)$, where different m correspond to different initial conditions with which these replicas start at $t=0$.

To apply WS theory, it is convenient to write equations for φ_j in complex form

$$\dot{\varphi}_m = \omega + \frac{\varepsilon}{N}\sum_{l\neq k}\sin\left(x_l-\varphi_m-\alpha\right) = \omega + \mathrm{Im}\left(H(t)\,\mathrm{e}^{-\mathrm{i}\varphi_m}\right), \quad H(t) = \frac{\varepsilon}{N}\sum_{l\neq k}\mathrm{e}^{\mathrm{i}(x_l-\alpha)}\,. \tag{22}$$

According to the WS theory, one introduces new variables ψ_j (WS phases) and complex WS amplitude z according to

$$\mathrm{e}^{\mathrm{i}\varphi_m} = \frac{z+\mathrm{e}^{\mathrm{i}\psi_m}}{1+z^*\mathrm{e}^{\mathrm{i}\psi_m}}\,. \tag{23}$$

Then, the WS equations for z,ψ_j are

$$\dot{z} = \mathrm{i}\omega z + \frac{1}{2}\left(H - H^* z^2\right)\,, \tag{24}$$

$$\dot{\psi}_m = \omega + \mathrm{Im}\left(z^* H\right)\,. \tag{25}$$

One can see that the relation of equation (25) for the WS phases are all the same, which means that there is in fact one nontrivial equation, and the differences of the WS phases are constants of motion (partial integrability).

The transformation of equation (23) is a Möbius transformation, and it is underdetermined. One can impose an additional condition at time $t=0$. It appears convenient to set $z(0)=0$, so that $\psi_m(0)=\varphi_m(0)$. If one introduces a variable Ψ which obeys equation (25) with initial condition $\Psi(0)=0$, i.e.

$$\dot{\Psi} = \omega + \mathrm{Im}\left(z^* H\right)\,, \tag{26}$$

then $\psi_m(t)=\varphi_m(0)+\Psi(t)$. This gives a solution of the system of equation (22) through the dynamics of z,Ψ:

$$e^{\mathrm{i}\varphi_m(t)} = \frac{z(t)+e^{\mathrm{i}(\varphi_m(0)+\Psi(t))}}{1+z^*(t)\,e^{\mathrm{i}(\varphi_m(0)+\Psi(t))}}\,. \tag{27}$$

It is more convenient to work with real variables J,β,γ, which we define as

$$H(t) = h(t)\exp\left[\mathrm{i}\Phi(t)\right], \quad z = \rho\exp\left[\mathrm{i}\left(\Phi+\beta\right)\right], \quad \Psi = \Phi+\beta+\gamma, \quad J = \frac{\rho^2}{2\left(1-\rho^2\right)}, \quad \rho = \sqrt{\frac{2J}{1+2J}}\,,$$

and rewrite the system of equations (24) and (26) together with equation (27) as a two-dimensional Hamiltonian system (where J is action and β is angle)

$$\begin{aligned}
\dot{J} &= \frac{\sqrt{2J(1+2J)}}{2}h(t)\cos(\beta) = -\frac{\partial \mathcal{H}(J,\beta)}{\partial \beta}\,,\\
\dot{\beta} &= \omega - \dot{\Phi}(t) - \frac{1+4J}{2\sqrt{2J(1+2J)}}h(t)\sin(\beta) = \frac{\partial \mathcal{H}(J,\beta)}{\partial J}\,,\\
\mathcal{H}(J,\beta) &= J\left[\omega - \dot{\Phi}(t)\right] - h(t)\,\frac{\sqrt{2J(1+2J)}}{2}\sin\beta\,,\\
\dot{\gamma} &= \frac{1}{2\sqrt{2J(1+2J)}}h(t)\sin(\beta)\,,\\
\exp\left[\mathrm{i}\varphi_m(t)\right] &= \exp\left[\mathrm{i}\left(\beta+\Phi(t)\right)\right]\frac{\sqrt{\frac{2J}{1+2J}}+\exp\left[\mathrm{i}\left(\varphi_m(0)+\gamma\right)\right]}{1+\sqrt{\frac{2J}{1+2J}}\exp\left[\mathrm{i}\left(\varphi_m(0)+\gamma\right)\right]}\,.
\end{aligned} \tag{28}$$

Let us focus on the dynamics at large times, where $J \gg 1$ (what corresponds to $\rho \approx 1$). In this limit the system of equation (28) reduces to

$$\dot{J} = Jh(t)\cos\beta = -\frac{\partial \tilde{\mathcal{H}}(J,\beta)}{\partial \beta}\,, \tag{29}$$

$$\dot{\beta} = \omega - \dot{\Phi}(t) - h(t)\sin\beta = \frac{\partial \tilde{\mathcal{H}}(J,\beta)}{\partial J}\,, \tag{30}$$

$$\tilde{\mathcal{H}}(J,\beta) = J\left(\omega - \dot{\Phi}(t) - h(t)\sin\beta\right)\,, \tag{31}$$

$$\dot{\gamma} = \frac{1}{4J}h(t)\sin(\beta)\,, \tag{32}$$

$$\tan\frac{\varphi_m(t)-\beta(t)-\Phi(t)}{2} = (8J)^{-1}\tan\frac{\varphi_m(0)+\gamma(t)}{2}\,, \tag{33}$$

where we used a formula $\exp[\mathrm{i}a] = (1+\mathrm{i}\tan(a/2))(1-\mathrm{i}\tan(a/2))^{-1}$ to write the Möbius transformation $\varphi_m(0) \to \varphi_m(t)$ in the real form.

Let us discuss properties of this solution, and implications for replica-attractor and replica-repeller.

1. We assume that $J \to \infty$ (or $\rho \to 1$) as $t \to \infty$, this is the condition for the existence of an attractor and a repeller. The growth rate of J follows from equation (29): $J \sim \exp[\mu t]$, where $\mu = \langle h(t)\cos\beta(t)\rangle$.
2. At large times where $J \gg 1$, according to equation (33), almost all initial phases $\varphi_j(0)$ converge to the attractor $\varphi(t) = \beta(t) + \Phi(t)$.
3. However, convergence to the attractor is ensured only outside a small vicinity of the point $\varphi_m(0) + \gamma(t) = \pi$. One can see that as $t \to \infty$, according to equation (32), $\gamma(t) \to \Gamma$ because the r.h.s. of equation (32) tends exponentially to zero. Thus, the initial condition $\varphi_m(0) = \pi - \Gamma$ does not converge to a replica-attractor, and therefore it produces a replica-repeller. Note that the exact initial position of the repeller can be obtained only after the whole trajectory for all $t > 0$ is known.
4. Stability of the attractor can be calculated by taking the derivative of the transformation of equation (33):

$$\frac{\mathrm{d}\varphi_m(t)}{\mathrm{d}\varphi_m(0)} = (8J)^{-1}\frac{\cos^2\frac{\varphi_m(t)-\beta(t)-\Phi(t)}{2}}{\cos^2\frac{\varphi_m(0)+\gamma(t)}{2}} = \frac{1+\tan^2\frac{\varphi_m(0)+\gamma(t)}{2}}{8J+(8J)^{-1}\tan^2\frac{\varphi_m(0)+\gamma(t)}{2}}. \tag{34}$$

   One can see that for all $\varphi_m(0)$ that are not close to $\pi - \gamma(t)$, the derivative $\frac{\mathrm{d}\varphi_m(t)}{\mathrm{d}\varphi_m(0)} \sim J^{-1}$. Defining the average stability of the trajectory (the negative Lyapunov exponent of the attractor) as $\Lambda_{\mathrm{attr}} = \lim_{t\to\infty}\frac{1}{t}\frac{\mathrm{d}\varphi_j(t)}{\mathrm{d}\varphi_m(0)}$, and taking into account that $J \sim \exp[\mu t]$, we get $\Lambda_{\mathrm{attr}} = -\mu = -\langle h(t)\cos\beta(t)\rangle$.
5. The instability of the repeller can be calculated by noting that the Möbius map, equation (33), can be inverted. We can simply invert the derivative of equation (34):

$$\frac{\mathrm{d}\varphi_m(0)}{\mathrm{d}\varphi_m(t)} = (8J)\frac{\cos^2\frac{\varphi_m(0)+\gamma(t)}{2}}{\cos^2\frac{\varphi_m(t)-\beta(t)-\Phi(t)}{2}} = (8J)^{-1}\frac{1+\tan^2\frac{\varphi_m(t)-\beta(t)-\Phi(t)}{2}}{(8J)^{-2}+\tan^2\frac{\varphi_m(t)-\beta(t)-\Phi(t)}{2}}. \tag{35}$$

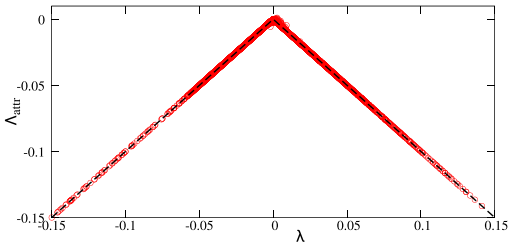

Figure 7. Test of the relation of equation (39) in a Kuramoto–Sakaguchi ensemble. Circles: calculated values of λ and Λ_{attr}; black dashed line: the relation of equation (39).

One can see that for all $\varphi_j(t)$ that are not close to $\beta(t)+\Phi(t)$ (i.e. are not close to the replica-attractor at time t), the derivative of the backward evolution $\frac{\mathrm{d}\varphi_m(0)}{\mathrm{d}\varphi_m(t)} \sim J^{-1}$. Because the evolution backward in time is concentrated at the replica-repeller, this shows that the Lyapunov exponent on the replica-repeller is $\Lambda_{\mathrm{rep}} = \mu = \langle h(t)\cos\beta(t)\rangle$. Comparing with equations (29) and (30), one can see that λ and $\Lambda_{\mathrm{attr}} = -\Lambda_{\mathrm{rep}}$ are two Lyapunov exponents of a Hamiltonian system, and their symmetry corresponds to the general symmetry of LEs in Hamiltonian dynamics.

Let us now discuss how the properties of the attractor and the repeller resulting from the WS theory are related to the originally introduced properties of the prototype and replicas. For this we rewrite the dynamics of the prototype x_k from equation (20) and its replica from equation (22), again omitting index k for simplicity

$$\dot{x} = \omega + h(t)\sin(\Phi(t) - x)\ , \tag{36}$$

$$\dot{\varphi} = \omega + h(t)\sin(\Phi(t) - \varphi)\ , \tag{37}$$

$$h\mathrm{e}^{\mathrm{i}\Phi} = \frac{\varepsilon}{N}\sum_{l\neq k}\mathrm{e}^{\mathrm{i}(x_l-\alpha)}\ . \tag{38}$$

Replica φ, initial condition of which is chosen 'randomly', almost always converges to an attractor, on which $\varphi(t) - \Phi(t) = \beta(t)$. Thus, stability of the replica is always given by $\Lambda_{\mathrm{attr}} = \langle h(t)\cos(\varphi(t) - \Phi(t))\rangle$.

Prototype x can lie on the repeller or on the attractor (in this case $x(t) \to \varphi(t)$ as $t \to \infty$). In the former case, it is unstable, and its transversal LE is $\lambda = -\langle h(t)\cos(x(t) - \Phi(t))\rangle = \Lambda_{\mathrm{rep}} = \mu > 0$. In the latter case, it is stable, and the transversal LE is $\lambda = -\langle h(t)\cos(x(t) - \Phi(t))\rangle = -\langle h(t)\cos(\varphi(t) - \Phi(t))\rangle = \Lambda_{\mathrm{attr}} = -\mu > 0$. Summarizing, we obtain the following symmetry relation between the stability of the replica Λ_{attr} and the LTLE of the prototype λ:

$$\Lambda_{\mathrm{attr}} = -|\lambda|\ . \tag{39}$$

We illustrate this relation in figure 7. Here we show values λ and Λ_{attr} for all units in an ensemble of $N = 21$ KS oscillators, equation (20), for all values of ε in the interval presented in figure 5 (only cases with $|\lambda| < 0.15$ are chosen for better visibility).

5. Conclusions

In summary, we have explored properties of internal reliability in a network of phase oscillators coupled via KS-type coupling. Reliability characterizes the 'stability' of the dynamics with respect to replicas of particular units; reliability means that all the replicas converge toward the prototype, while in an anti-reliable case, replicas converge to a different state. The presence of reliable and anti-reliable units appears to be a generic feature in a wide range of system sizes and dynamical regimes. For two coupled oscillators, reliability properties have been calculated analytically. Here, in a general situation, in the asynchronous state, one oscillator is reliable and another one anti-reliable. This situation can also be observed in the synchronous state, although in some regions of parameters, both oscillators are reliable.

The case of KS phase oscillators is particular, because a set of replicas possesses one attracting and one repelling trajectory. We speak here about 'replica-attractor' and 'replica-repeller', not to be confused with attractors and repellers in the original system. Therefore, one can interpret a reliable unit as one staying on the replica-attractor, while in an anti-reliable case, the prototype stays on the replica-repeller. Furthermore, there is an interesting symmetry between replica-attractor and replica-repeller following

from the WS description of the dynamics of KS oscillators: their stability exponents have the same value but opposite signs.

Acknowledgments

FB wishes to thank the University of Perpignan Via Domitia for kind hospitality. SI acknowledges financial support from the Italian MUR PRIN2022 project "Breakdown of ergodicity in classical and quantum many-body systems" (BECQuMB) Grant No. 20222BHC9Z.

Data availability statement

All data that support the findings of this study are included within the article (and any supplementary files).

Author contributions

Arkady Pikovsky 0000-0001-9682-7122
Conceptualization (lead), Data curation (equal), Formal analysis (lead), Funding acquisition (equal), Investigation (lead), Methodology (lead), Project administration (equal), Software (lead), Supervision (equal), Validation (lead), Visualization (lead), Writing – original draft (lead), Writing – review & editing (equal)

Franco Bagnoli 0000-0002-6293-0305
Conceptualization (equal), Formal analysis (equal), Funding acquisition (equal), Investigation (equal), Validation (equal), Writing – original draft (equal), Writing – review & editing (equal)

Stefano Iubini 0000-0002-0157-8176
Conceptualization (equal), Formal analysis (equal), Investigation (equal), Methodology (equal), Software (equal), Writing – original draft (equal), Writing – review & editing (equal)

References

[1] Pikovsky A S 1984 Synchronization and stochastization of the ensemble of autogenerators by external noise *Radiophys. Quantum Electron.* **27** 390–5
[2] Mainen Z F and Sejnowski T J 1995 Reliability of spike timing in neocortical neurons *Science* **268** 1503
[3] Ermentrout G B, Galán R F and Urban N N 2008 Reliability, synchrony and noise *Trends Neurosci.* **31** 428–34
[4] Teramae J and Fukai T 2007 Reliability of temporal coding on pulse-coupled networks of oscillators (arXiv:0708.0862)
[5] Lin K K, Shea-Brown E and Young L S 2009 Reliability of coupled oscillators *J. Nonlinear Sci.* **19** 497–545
[6] Goldobin D S and Pikovsky A 2006 Antireliability of noise-driven neurons *Phy. Rev. E* **73** 061906
[7] Stanley H E, Stauffer D, Kertesz J and Herrmann H J 1987 Dynamics of spreading phenomena in two-dimensional Ising models *Phys. Rev. Lett.* **59** 2326
[8] Herrmann H 1990 Damage spreading *Physica A* **168** 516–28
[9] Grassberger P 1995 Are damage spreading transitions generically in the universality class of directed percolation? *J. Stat. Phys.* **79** 13–23
[10] Bagnoli F and Rechtman R 1999 Synchronization and maximum Lyapunov exponents of cellular automata *Phys. Rev. E* **59** R1307
[11] Rulkov N F, Suschik M M, Tsimring L S and Abarbanel H D I 1995 Generalized synchronization of chaos in directionally coupled chaotic systems *Phys. Rev. E* **51** 980
[12] Abarbanel H D, Rulkov N F and Sushchik M M 1996 Generalized synchronization of chaos: the auxiliary system approach *Phys. Rev. E* **53** 4528
[13] Baia M, Bagnoli F, Matteuzzi T and Pikovsky A 2025 Synchronization of branching chain of dynamical systems *Physica D* **477** 134664
[14] Letellier C, Sendiña-Nadal I, Leyva I and Barbot J P 2023 Generalized synchronization mediated by a flat coupling between structurally nonequivalent chaotic systems *Chaos* **33** 093117
[15] Letellier C, Minati L, Sendina-Nadal I and Leyva I 2024 A taxonomy for generalized synchronization between flat-coupled systems (arXiv:2401.11561)
[16] Matteuzzi T, Bagnoli F, Baia M, Iubini S and Pikovsky A 2025 Internal reliability and antireliability in dynamical networks *Phys. Rev. E* **112** 044216
[17] Pecora L M and Carroll T L 1990 Synchronization in chaotic systems *Phys. Rev. Lett.* **64** 821–4
[18] Sakaguchi H and Kuramoto Y 1986 A soluble active rotator model showing phase transition via mutual entrainment *Prog. Theor. Phys.* **76** 576–81
[19] Acebrón J A, Bonilla L L, Vicente C J P, Ritort F and Spigler R 2005 The Kuramoto model: a simple paradigm for synchronization phenomena *Rev. Mod. Phys.* **77** 137–75

[20] Chen B, Engelbrecht J R and Mirollo R 2019 Dynamics of the Kuramoto-Sakaguchi oscillator network with asymmetric order parameter *Chaos: Interdiscip. J. Nonlinear Sci.* **29** 013126
[21] Gupta S, Campa A and Ruffo S 2018 *Statistical Physics of Synchronization* (Springer)
[22] Watanabe S and Strogatz S H 1993 Integrability of a globally coupled oscillator array *Phys. Rev. Lett.* **70** 2391–4
[23] Watanabe S and Strogatz S H 1994 Constants of motion for superconducting Josephson arrays *Physica D* **74** 197–253
[24] Pikovsky A and Politi A 2016 *Lyapunov Exponents: a Tool to Explore Complex Dynamics* (Cambridge University Press)
[25] Hong H and Strogatz S H 2011 Kuramoto model of coupled oscillators with positive and negative coupling parameters: an example of conformist and contrarian oscillators *Phys. Rev. Lett.* **106** 054102
[26] Hong H and Strogatz S H 2011 Conformists and contrarians in a Kuramoto model with identical natural frequencies *Phys. Rev. E* **84** 046202
[27] Popovych O V, Maistrenko Y L and Tass P A 2005 Phase chaos in coupled oscillators *Phys. Rev. E* **71** 065201
[28] Maistrenko Y L, Popovych O V and Tass P A 2005 Chaotic attractor in the Kuramoto model *Int. J. Bifurc. Chaos* **15** 3457–66
[29] Carlu M, Ginelli F and Politi A 2018 Origin and scaling of chaos in weakly coupled phase oscillators *Phys. Rev. E* **97** 012203
[30] Brister B N, Belykh V N and Belykh I V 2020 When three is a crowd: chaos from clusters of Kuramoto oscillators with inertia *Phys. Rev. E* **101** 062206
[31] Marvel S A, Mirollo R E and Strogatz S H 2009 Phase oscillators with global sinusoidal coupling evolve by Mobius group action *Chaos* **19** 043104
[32] Pikovsky A and Rosenblum M 2015 Dynamics of globally coupled oscillators: progress and perspectives *Chaos* **25** 097616
[33] Braun W, Pikovsky A, Matias M A and Colet P 2012 Global dynamics of oscillator populations under common noise *EPL* **99** 20006